Neuro-Oncology 14(4):459–470, 2012.
doi:10.1093/neuonc/nor231
Advance Access publication February 3, 2012

Oncolytic measles virus prolongs survival in a murine model of cerebral spinal fluid–disseminated medulloblastoma

Adam W. Studebaker, Brian Hutzen, Christopher R. Pierson, Stephen J. Russell, Evanthia Galanis, and Corey Raffel

The Center for Childhood Cancer, The Research Institute at Nationwide Children's Hospital, Columbus, Ohio (A.W.S., B.H.); Molecular, Cellular, and Developmental Biology Program (B.H.); Department of Pathology, The Ohio State University College of Medicine, Columbus, Ohio (C.R.P.); Department of Molecular Medicine (S.J.R.); Division of Medical Oncology, Mayo Clinic, Rochester, Minnesota (E.G.); Department of Neurological Surgery, The Ohio State University College of Medicine, Columbus, Ohio (C.R.)

Medulloblastoma is the most common malignant brain tumor of childhood. Although the survival rate of afflicted children has improved considerably over the past several years, a subset of these patients will present with disseminated disease and face a much bleaker prognosis. In addition, patients may present with disseminated disease at recurrence. We previously demonstrated the efficacy of a recombinant oncolytic measles virus (MV) to treat localized medulloblastoma in a mouse xenograft model. In the present study, we sought to extend our findings to the treatment of disseminated disease. To this end, we developed and characterized a mouse xenograft model of disseminated medulloblastoma using serial bioluminescent imaging techniques in combination with histopathological examination. Mice injected with medulloblastoma cells into their right lateral ventricle showed tumor growth in their ventricles and in both intracranial and spinal subarachnoid spaces, closely recapitulating the human disease. Subsequent intraventricular administration of MV resulted in stabilization and shrinkage of the tumor, significantly prolonging the survival of the treated animals, compared with those treated with an inactivated virus. These data demonstrate that oncolytic MV may be of use in treating disseminated medulloblastoma. In addition, our protocol of intraventricular tumor cell injection, followed by bioluminescent imaging coupled with histopathological examination, provides a model for use in evaluating future recombinant oncolytic viruses and other preclinical therapeutic approaches for disseminated medulloblastoma.

Keywords: bioluminescence, dissemination, measles virus, medulloblastoma, oncolytic virus.

Medulloblastoma is the most common malignant brain tumor of childhood, accounting for 15% to 20% of all pediatric brain tumors.[1] Approximately 350–400 new cases are diagnosed annually in the United States.[2] Using current multimodality treatment consisting of surgery, craniospinal radiotherapy, and multiple drug chemotherapy, the 5-year survival rate is now ~60%.[3,4] However, many children receiving this therapy experience long-term treatment-related morbidity, which greatly affects their quality of life.[5–8] Although a number of prognostic factors influence survival, dissemination of tumor into the cerebrospinal fluid (CSF) pathways, present in ~20% of patients at initial diagnosis and in ~75% of patients at recurrence, is an especially grave negative prognostic factor.[9–11] Fewer than 20% of children presenting with CSF dissemination live for 5 years.[12] Clearly, more effective therapy for medulloblastoma and, in particular, for disseminated medulloblastoma is needed.

Medulloblastomas predominantly arise in the fourth ventricle between the cerebellar vermis and brainstem, often leading to occlusion of the ventricle and subsequent hydrocephalus.[13] Because of the aggressive nature of medulloblastoma and its close proximity to the CSF, patients may present with disseminated disease in the ventricles, basal cisterns, and/or spinal

Received September 14, 2011; accepted December 12, 2011.

Corresponding Author: Corey Raffel, MD, PhD, Department of Neurological Surgery, The Ohio State University College of Medicine, 400 W. 12th St., Wiseman Hall 385, Columbus, OH 43210 (corey.raffel@osumc.edu).

subarachnoid space.[9–11] Previous studies have demonstrated dissemination of human medulloblastoma cell lines in murine orthotopic models when tumor cells were injected either into the subarachnoid space of the cisterna magna[14] or cerebellum.[15,16] In both models, pathological review revealed tumor involvement in the ventricular system and the spinal cord.

We recently reported on the therapeutic efficacy of a recombinant Edmonston's vaccine strain of measles virus (MV) against a panel of human medulloblastoma cell lines in vitro and in a mouse orthotopic model of medulloblastoma.[17] In these studies, both irradiated SCID and athymic nude mice implanted with human medulloblastoma cell lines in the caudate putamen demonstrated significantly increased survival when treated with a recombinant MV, compared with those mice treated with a UV-inactivated form of the virus. In the current study, we sought to develop a mouse model that recapitulated the dissemination pattern exhibited by children with medulloblastoma and, thus, determine whether a similar therapeutic approach using recombinant MV would increase animal survival.

In this study, we demonstrate a pattern of human medulloblastoma dissemination in a murine model that is similar to the dissemination pattern exhibited by children with the disease. Unlike the previous studies requiring necropsy to demonstrate CSF-disseminated disease,[14–16] our model was capable of using intravital bioluminescent imaging to evaluate dissemination. Subsequent necropsy revealed extensive intraventricular and subarachnoid disease involving both the extra-cerebral and spinal subarachnoid spaces, thus confirming our imaging data. In many cases, these animals also exhibited hydrocephalus resulting from blockage of CSF flow. Of more importance, we found that the animals treated with a modified MV exhibited morphologic and immunohistochemical evidence of viral infection of tumor cells throughout the CSF and statistically increased survival times relative to controls. We have demonstrated effective treatment of disseminated medulloblastoma with MV in a new murine model of CSF dissemination. Ongoing experiments in our laboratory to determine optimal dosing of virus in preparation for a phase I trial are under way.

Material and Methods

Cell Culture

The Vero (African green monkey) and D283med human medulloblastoma cell lines were obtained from the American Type Culture Collection. The D425med human medulloblastoma cell line was obtained from Darrell Bigner (Duke University, Durham, NC). Vero and medulloblastoma cells were grown in DMEM supplemented with 10% or 20% fetal bovine serum, respectively, at 37°C in a humidified incubator set at 5% CO_2. The D283med- and D425med-Luciferase cell lines were generated using a method previously described.[17] Luciferase bioluminescence emitted per cell line was quantified. D283med-luciferase (D283luc) and D425med-luciferase (D425luc) cells (5×10^4) were plated in replicates of 6 in a well of a white 96-well plate. Twenty-four hours later, Bright-Glo reagent (Promega) was added to each well. A Victor2 Wallac plate reader (Perkin Elmer) was used to measure light emissions in counts per second over a 10-s period. Data were quantified as counts per second per cells.

Production of Measles Virus

The MV-GFP virus was rescued as described elsewhere[18] and propagated in Vero cells by infecting them at a multiplicity of infection of 0.01 for 2 h at 37°C in a minimal volume of Opti-MEM (Invitrogen). After incubation, the medium containing unabsorbed virus was replaced with DMEM supplemented with 10% fetal bovine serum. Cells were incubated for 48 h at 37°C and then transferred to 32°C for 24 h. The presence of eGFP-positive cells was verified by fluorescence microscopy. Medium was gently aspirated, and cells were collected in Opti-MEM. Virus was harvested by 2 cycles of freezing and thawing. The titer of the virus was determined by 50% tissue culture infective dose ($TCID_{50}$) titration on Vero cells.[19]

In Vivo Disseminated Tumor Model

D283luc (1×10^6 cells) or D425luc (5×10^5 cells) were injected into the right lateral ventricle of 5-week-old Hsd:Athymic Nude-*Foxn1nu* mice (Harlan Laboratories) using the small animal stereotactic frame (David Kopf Instruments). The injection coordinates were 1 mm to the right and 0.5 mm posterior to the bregma and 2.2 mm below the skull surface. The mice were kept under isoflurane gas anesthesia while cells in phosphate-buffered saline were injected over a course of 3 min using a 26-guage Hamilton syringe. These mice were randomly divided into groups for treatment with MV-GFP (MV) or an UV-inactivated form of the virus (UV-MV). Treatment regimens were initiated either 3 or 14 days after tumor implantation, with each mouse receiving an injection of 2×10^5 $TCID_{50}$ of MV or UV-MV at the same stereotactic coordinates used for implantation. Treatments were repeated every other day for a total of 5 doses (1×10^6 total $TCID_{50}$). The animals were euthanized if they developed neurologic deficits, such as hemiparesis or lethargy. All animal experiments were approved by the Nationwide Children's Hospital Institutional Animal Care and Use Committee.

Histopathological Evaluation

At the time of necropsy, brains and spinal columns were collected, fixed overnight with 10% formalin, paraffin embedded, cut into 4-μm tissue sections, and

stained with hematoxylin and eosin. The spinal cords were placed in decal solution (Formical-2000; Decal Chemical) overnight following formalin fixation and prior to paraffin embedding. The D283luc tumor focus isolated in the spinal cord of the animal 3 days following tumor implantation was visualized using a Zeiss Axioskop 2 Plus microscope and photographed using a Zeiss AxioCam MRc 5 camera. Individual cells in the focus were counted, and the radius of individual cells and the entire focus were determined using the AxioVs40 V 4.6.3.0 morphometry. The radius value of 10 independent cells was calculated to determine the average radius. Four radius measurements were taken of the entire tumor focus to determine an average radius. From these values, the volume of the individual cells and the entire focus was determined. These values allowed us to calculate the number of cells in the tumor focus.

Immunohistochemistry of Medulloblastoma Tumor Xenografts

To confirm intratumor MV infection, measles nucleoprotein was detected by immunohistochemistry of paraffin-embedded tissue sections obtained from D283luc and D425luc xenografts. Following tumor cell implantation, a single MV treatment was administered 7 days following tumor implantation using the same stereotaxic techniques previously described. Tissues were collected 48 h following MV treatment and prepared as described above. Formalin-fixed paraffin-embedded samples were sectioned with a microtome (Finesse; Thermo Scientific) at 4 μm, placed on charged slides, oven dried, deparaffinized, and hydrated with distilled water. Heat-induced epitope retrieval was performed by immersing the slide in antigen retrieval solution (sodium citrate buffer; pH, 6.0) and placed in a decloaking chamber for 30 min at 120°C. Slides were cooled and then rinsed with distilled water. To block endogenous peroxidase activity, slides were incubated in 3% hydrogen peroxide for 15 min. After rinsing with distilled water, slides were washed with Tris-buffered saline solution with Tween 20 (TBST). To reduce nonspecific background, slides were incubated in super block (ScyTek Laboratories) for 10 min and then washed with TBST. The slides were then incubated in the primary antibody, anti-measles nucleoprotein antibody (NB100–1856; Novus Biologicals), at a 1:300 dilution for 1 h and then rinsed with TBST. Next, slides were incubated in UltraTek Anti-Polyvalent Biotinylated Antibody (ScyTek Laboratories) for 10 min. After washing in TBST, the slides were incubated in UltraTek HRP (ScyTek Laboratories) for 10 min. Slides were then washed in TBST, incubated in substrate (AEC Chromagen, ScyTek Laboratories) for 3.5 min, counter stained with hematoxylin (Shandon Gill; Thermo Scientific), and blued using ammonia water. From distilled water, the sections were coated with crystal mounting media, heated at 58°C, and cover slipped with Permount mounting media. For comparison, additional sections were cut from samples positive for intratumor MV infection and tested with the same immunostaining procedure, with the exception of the primary antibody. Modified versions of the immunohistochemical protocol described above were used to evaluate xenograft tissue for cell proliferation and apoptosis. Slides prepared as described above were either incubated in the primary antibody Ki-67 (VP-K451; Vector Laboratories) at a 1:1000 dilution for 1 h to detect proliferation or in the primary antibody cleaved caspase-3 (Asp175; 96661; Cell Signaling) at a 1:200 dilution for 1 h to detect apoptosis. After the slides were rinsed with TBST, the Ki-67 slides were incubated in 4+ Biotinylated Universal Goat Link (Biocare Medical) for 10 min, washed with TBST, and incubated in 4+ Streptavidin HRP (Biocare Medical) for 10 min. The cleaved caspase-3 slides were incubated in UltraTek Anti-Polyvalent Biotinylated Antibody for 10 min. After washing in TBST, the slides were incubated in UltraTek HRP (ScyTek Laboratories) for 10 min. Slides were then washed in TBST, incubated in substrate (DAB, Vector Laboratories) for 30 s, counter stained with hematoxylin (Shandon Gill; Thermo Scientific), and blued using ammonia water.

In Vivo Bioluminescence Imaging

For the studies characterizing tumor dissemination and growth, bioluminescence imaging was conducted on days 3, 7, 14, and 21 for D283luc and days 3 and 10 for D425luc following tumor implantation. In studies evaluating the efficacy of MV therapy, bioluminescence imaging was performed prior to each MV injection, then weekly thereafter. Bioluminescence imaging was conducted using the Xenogen IVIS Spectrum (Caliper Life Sciences). Animals received an intraperitoneal injection of 4.5 μg Xenolight Rediject D-Luciferin (Caliper Life Sciences) and were continuously maintained under isoflurane gas anesthesia. Images were obtained 20 min after luciferin administration. The bioluminescence intensity was quantified in units of photons per second using Living Image Software (version 4.1; Caliper Life Sciences). The lower threshold of detection was set at 1250 photons/s/cm^2/sr.

Statistical Analysis

Survival curves were generated using the Kaplan-Meier method and GraphPad Prism 5 software (GraphPad Software). Statistical significance ($P < .05$) between the groups was determined using the log-rank test. All other statistical analysis was performed using Microsoft Office Excel (v.11.6560.6568 SP2) in Data Analysis using Regression or Student's *t* test: paired 2-sample for means. Probabilities for the Student's *t* test are listed as "P(T ≤ t) 2-tail" with an α of 0.05.

Results

Medulloblastoma Cell Line Dissemination and Growth at Distant Sites Can Be Detected by Intravital Bioluminescence

To evaluate whether MV therapy would be effective at treating disseminated medulloblastoma, we first planned to determine whether we could establish a model of CSF dissemination. We previously demonstrated that we could follow localized tumor growth and treatment efficacy in vivo using bioluminescent imaging techniques[17] and wanted to determine whether this imaging modality would also be suitable for visualizing disseminated disease. Using stereotaxic guidance, we initially injected D283med cells stably expressing firefly luciferase (D283luc) into the lateral ventricles of athymic nude mice, where the cells would have direct access to the CSF. Successful implantation of D283luc cells and their subsequent dissemination were confirmed with bioluminescent imaging prior to initiating MV treatment (Fig. 1A and B). An animal with a bioluminescent signal >1250 photons/s/cm^2/sr in its spinal cord was determined to have successful dissemination (Fig. 1B). This setting was chosen because it is substantially higher than the documented background auto-luminescence of a nude mouse (1000 photons/s/cm^2/sr).[20] Using this technique to evaluate dissemination, we determined our success rate to be 83.4% (126 of 151 animals), with an average spinal cord signal intensity of 1.47×10^4 ($0.250–5.47 \times 10^4$) photons/s/cm^2/sr. Animals displaying disseminated tumor on day 3 were additionally imaged on days 7, 14, and 21 after tumor implantation. As shown in Fig. 1A and B, the bioluminescent signal in both the brain and the spinal cord increases over time, as evaluated by total flux of the bioluminescent signal. Of interest, those animals implanted with D283luc and not displaying a bioluminescent signal in their spinal cords 3 days following tumor implantation never developed a signal throughout the course of evaluation (21 days). For this reason, animals not showing signal in the spine prior to treatment were not used in subsequent studies.

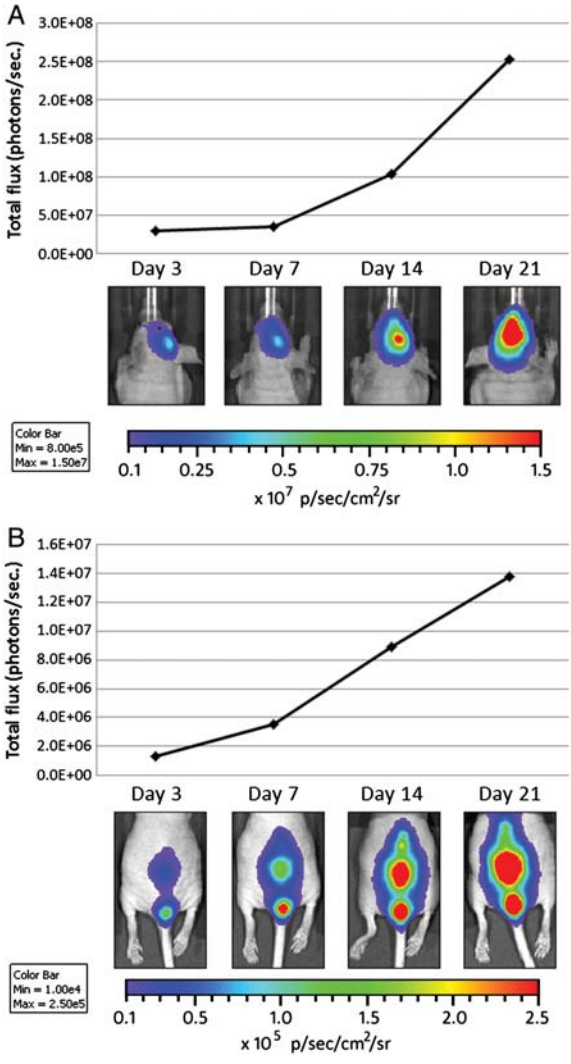

Fig. 1. In vivo evaluation of medulloblastoma dissemination and disease progression. Bioluminescence images from mice containing D283Luc tumors. Animals were implanted with D283luc cells in the right lateral ventricle. Bioluminescence imaging was conducted 3, 7, 14, and 21 days following tumor implantation. Bioluminescent signals in the brain and spinal cord are visible as early as 3 days following tumor implantation. Tumor burden in the brain and spinal cord, as determined by total flux (photons/s), increased steadily over time. Animals not displaying a bioluminescent signal in their spinal cord at day 3 failed to exhibit a signal throughout the course of the study and were excluded from the study (data not shown).

Murine Model of Medulloblastoma Dissemination Closely Models the Pattern Observed in Children

To confirm the dissemination pattern of D283luc in animals following introduction of tumor cells into the lateral ventricle, animals were euthanized following bioluminescent imaging. Histopathological review of the entire brain and spinal cord confirmed an animal's corresponding imaging data. Animals that displayed a bioluminescent signal in their spinal cord also were found to have tumor in their spinal cord following microscopic review (Fig. 2). Furthermore, animals exhibiting disseminated disease revealed extensive intraventricular and intracranial subarachnoid disease (Fig. 2A). By examining serial sections from the spinal cord of the animal displaying a positive bioluminescent signal 3 days following tumor implantation (Fig. 2; inset), we were able to determine that there were approximately 3000 D283luc cells within the tumor focus. As expected, animals euthanized 14 days post tumor implantation and after displaying endpoint symptoms had increased tumor burden and severity of dissemination, including tumor foci located around the cerebellum and brain stem (Fig. 2A). Conversely, animals that failed to display a bioluminescent signal in their spinal cord were found not to have

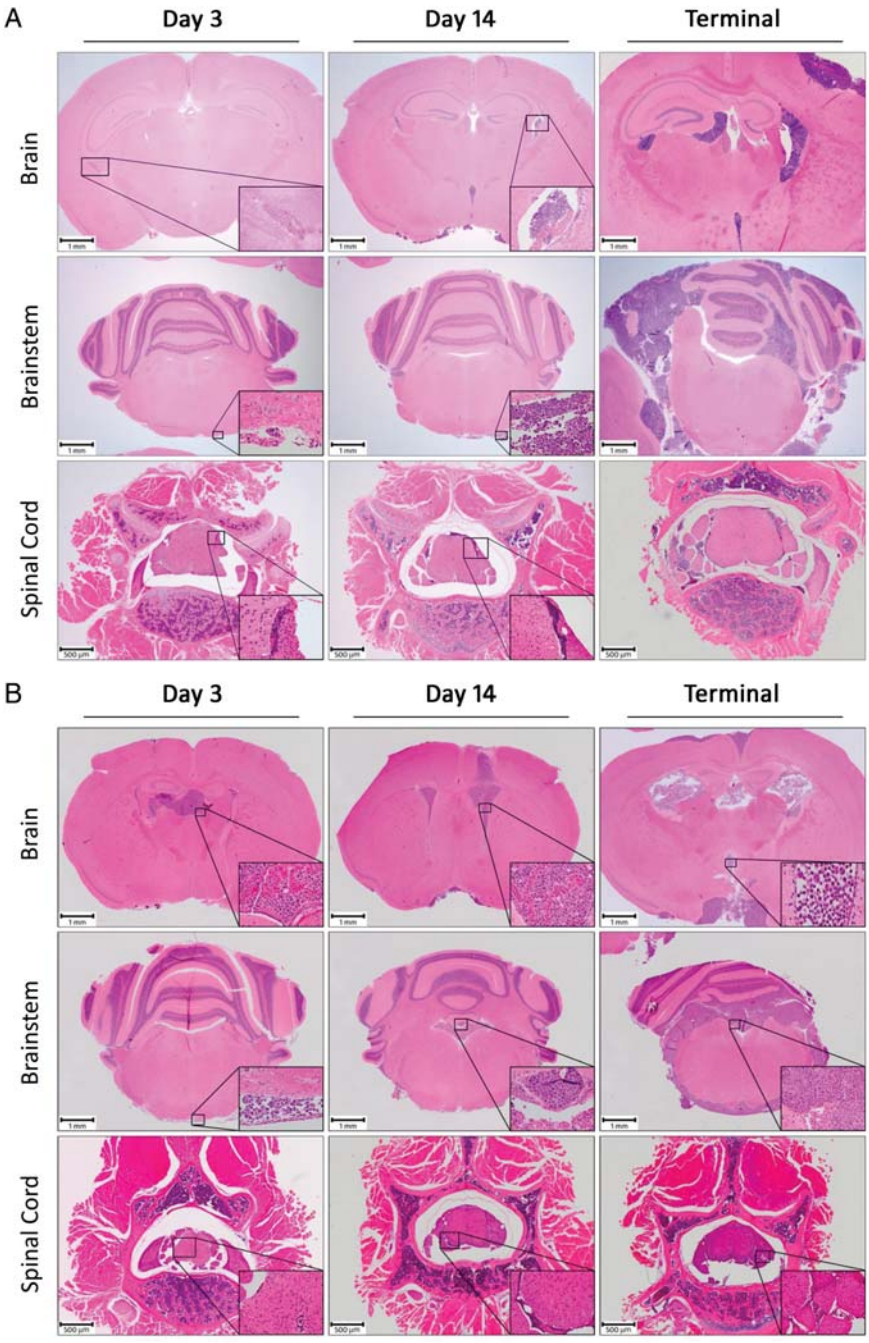

Fig. 2. Histological examination (H&E stain) of the mouse brain following injection of medulloblastoma cells into the right lateral ventricle of the mouse brain. (A) The presence of a D283luc-derived tumor in the ventricle, posterior fossa, and spinal cord is demonstrated as early as 3 days following tumor implantation. There is a temporal increase in the extent of dissemination and tumor burden following tumor implantation. Tumor is present in the intraventricular and intracranial subarachnoid spaces, especially the cerebellum and brain stem. Tumor is evident in the sacral region of the spinal cord as well. Evaluation of an animal following terminal disease revealed extensive intraventricular and intracranial subarachnoid space involvement. The ventricles appear occluded by tumor, and the cerebellum has extensive disease. Tumor has invaded the dorsal root ganglia as well as the spinal cord. All insets were originally taken at × 400. (B) Similar observations are found in disseminated tumors of the D425luc-derived cell line.

histopathologic evidence of disease in their spinal cord, intraventricular space, or subarachnoid space. These animals had a tumor mass in the caudate putamen, indicating that the tumor cells may not have been properly implanted into the lateral ventricle (data not shown).

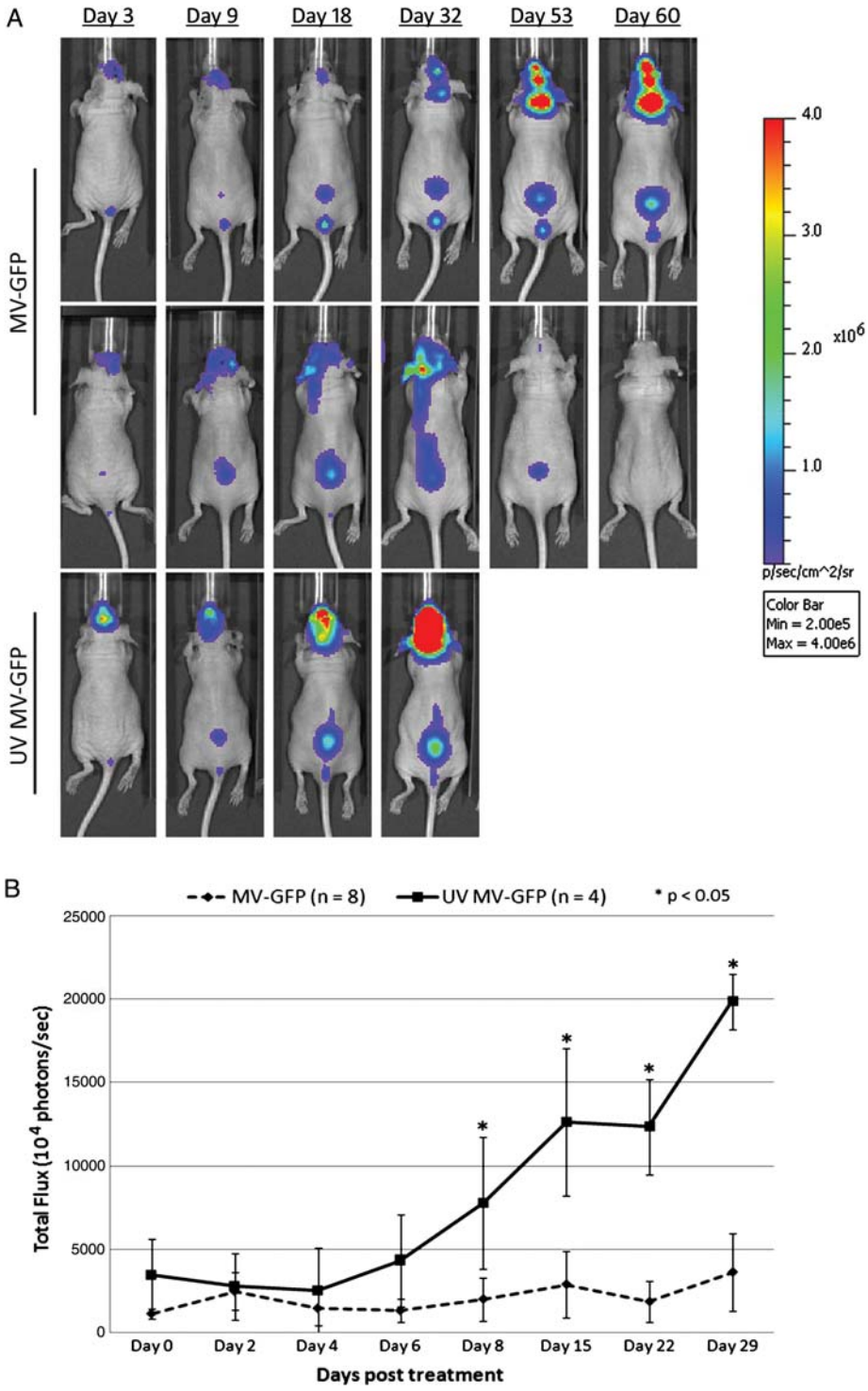

Fig. 3. In vivo evaluation of antitumor activity of measles virus (MV). Bioluminescent images from mice containing D283Luc tumors. Animals were implanted with D283luc cells in the right lateral ventricle 3 days prior to treatment. MV treatment was administered on days 0, 2, 4, 6, and 8. Bioluminescence signal in the lower vertebral region is indicative of tumor dissemination. (A) One MV-treated animal exhibits complete tumor abolition, as determined by the lack of bioluminescent signal in the spinal cord (day 60). The other MV-treated animal exhibits a delayed increase in tumor burden compared to the untreated animal, which displays significant temporal increase in tumor burden. (B) MV-treated animals display a delayed progression of tumor burden compared to untreated animals when using total flux (photons/s) as an indicator of tumor burden.

Administration of Measles Virus Directly into the CSF Increases Survival of Mice Exhibiting Disseminated Medulloblastoma Tumors

To determine the efficacy of MV treatment in our model of disseminated disease, we established D283luc xenografts in athymic nude mice. Fourteen days following tumor implantation, we began a treatment regimen by injecting MV into the right lateral ventricle every other day for 10 days. The animals were then monitored to assess survival. There was a small but significant increase in survival of animals treated with MV, compared with animals treated with UV-MV ($P < .002$) (Fig. 4A). The median survival for MV-treated animals was 49 days (range, 47–49 days), compared with 40 days (range, 37–42 days) for UV-MV–treated animals. There were no long-term survivors in the MV treatment group. Pathological review determined that all 5 UV-MV–treated animals had extensive intraventricular, intracranial subarachnoid space, and spinal cord involvement. Likewise, all 5 MV-treated animals displayed ventricular and subarachnoid disease, but we were unable to detect tumor in the spinal cords of 2 animals.

We noted from our histopathological review that the tumor burden in the CSF was already quite large by 14 days after injection (Fig. 2A). On the basis of this finding and the survival results, we were concerned that the large burden of tumor in the subarachnoid space at 14 days after tumor injection was preventing the injected virus from moving through the subarachnoid space to access the entire tumor. To address this concern, we modified the experiment described above by beginning treatment 3 days after intraventricular injection of tumor cells. As before, the animals received a dose of MV every other day for a total of 5 injections of MV. Animals were followed up with serial imaging (Fig. 3) and monitored to assess survival. Quantification of photons released by D283luc-implanted tumors demonstrated that tumors either stabilized or shrank in treated animals, compared with UV-MV–treated animals (Fig. 3B). Two of 8 treated animals appeared to have been cured of disseminated disease, as determined by bioluminescent imaging (Fig. 3). There was statistically significant prolongation of survival in MV-treated mice, compared with UV-inactivated virus-treated controls ($P < .0005$) (Fig. 4B). UV-MV–treated animals had a median survival of 37 days (range, 35–39 days), whereas MV-treated animals had a median survival of 82 days (range, 64–110 days). A second independent study also demonstrated a significant increase in survival ($P < .0009$; data not shown). In that study the median survival of MV-treated mice was 83.5 days (range, 66–104 days), compared with 38.5 days (range, 35–42 days) for mice treated with UV-MV. Necropsy revealed extensive intraventricular, intracranial subarachnoid, and spinal subarachnoid disease in both treated and untreated animals (Fig. 2). The 2 animals devoid of any bioluminescent signal in the first study were free of disease upon pathological evaluation of their brains and spinal cords (data not shown). Two additional animals in the second study were also devoid of tumor upon pathological examination (data not shown).

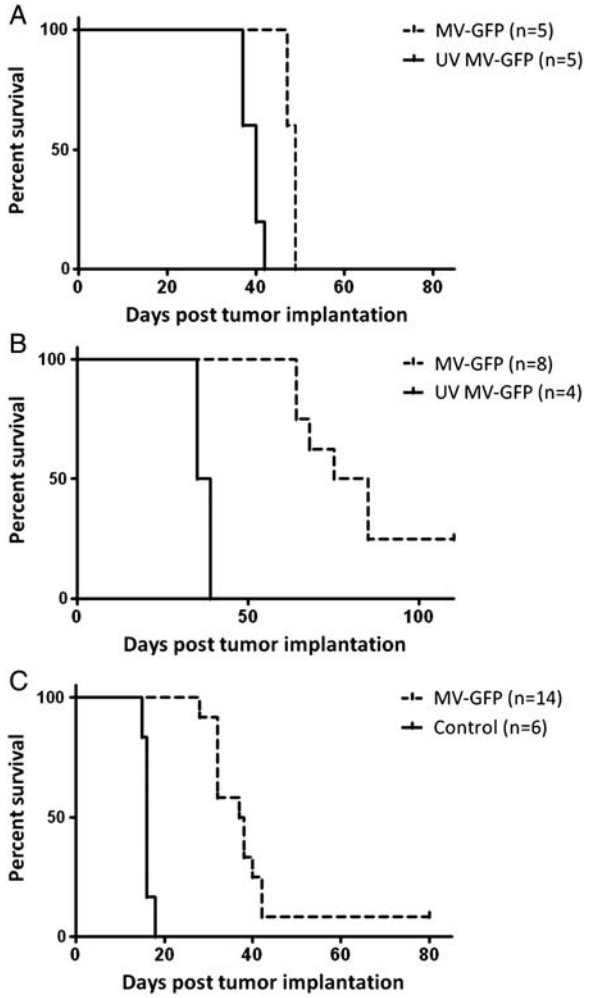

Fig. 4. Antitumor effect of measles virus (MV). D283luc medulloblastoma cells were injected into the right lateral ventricle of female athymic nude mice. Fourteen days (A) or 3 days (B) post tumor implantation the mice received a total of 1×10^6 pfu of MV or the same dose of UV-MV. Mice treated with MV had significantly longer survival than mice that received UV-MV ($P < .002$ (A); $P < .0005$ (B)). Mice treated with MV 14 days after tumor implantation had a median survival time of 49 days compared to 40 days exhibited by the UV-MV mice. Likewise, mice treated with MV-GFP 3 days after tumor implantation had a median survival time of 80 days, whereas the UV MV-GFP mice had a median survival time of only 37 days. (C) A similar experiment also demonstrated significant ($P < .0001$) survival of mice treated with MV 3 days following D425luc implantation when compared to mice that received UV-MV-GFP. D425luc xenografts treated with MV had a median survival time of 37.5 compared to 16 days for xenografts treated with UV-MV.

Dissemination and Treatment of D425med Tumor Xenografts

Because of the heterogeneous nature of medulloblastoma,[21] we constructed a second medulloblastoma luciferase-expressing cell line, D425luc, to evaluate its dissemination pattern when delivered directly into the CSF and to determine whether MV therapy would be efficacious against another cell line. In contrast to D283luc, the bioluminescent signal in the spinal cord of animals implanted with D425luc was delayed, occasionally taking as long as 10 days to visualize. In vitro evaluation of the 2 cell lines revealed that D283luc cells emitted 10-fold more counts/s/cell than did D425luc cells (350–400 counts/s/cell vs 35–40 counts/s/cell). Of interest, the average spinal cord signal intensity in D425luc xenografts when first detected was 1.47×10^3 ($1.33–1.97 \times 10^3$) photons/s/cm^2/sr, which is 10-fold lower than the initial intensity observed with D283luc xenografts.

Although some animals implanted with D425luc failed to display a bioluminescent signal in their spinal cord until day 10, histopathological review was still performed on days 3 and 14 following tumor implantation. Similar to what was observed with D283luc, animals either displayed progressive intraventricular and intracranial subarachnoid disease (Fig. 2B), characteristic of disseminated disease, or a primary tumor in the caudate putamen indicating a failed implantation. Using histopathological evaluation, we determined that 81.3% (39 of 48 animals) had disseminated tumor, a percentage very similar to our efficiency with D283luc. Animals implanted with D425luc appear to have greater tumor burden than the day-matched D283luc animals, including more widespread spinal cord distribution and ventricle occlusion, consistent with the more rapid growth rate of this cell line in vitro (Fig. 2B).

A similar treatment approach was performed in mice with established D425luc xenografts. An initial study evaluating MV efficacy initiated 14 days after tumor implantation could not be completed, because animals implanted with D425luc displayed clinical symptoms of disease prior to completing the treatment regimen. As with the second generation D283luc xenograft study, efficacy of MV treatment against disseminated D425luc was evaluated with treatment commencing 3 days after tumor implantation. Animals received either a dose of MV or a dose of UV-MV every other day for a total of 5 doses. Animals treated with MV had a significantly longer survival than did animals treated with the UV-MV ($P < .0001$) (Fig. 4C). UV-MV–treated animals had a median survival of 16 days (range, 15–18 days), whereas MV-treated animals had a median survival of 37.5 days (range, 32–80 days). One animal that displayed disseminated disease prior to initiating MV treatment was determined by bioluminescent imaging to be tumor free when euthanized on day 80. Histopathological evaluation of this animal failed to detect any tumor. In contrast, all other animals revealed extensive intraventricular, intracranial, and spinal subarachnoid disease (Fig. 2B). Because bioluminescent imaging evaluation prior to initiating treatment was proven to be unreliable with D425luc, because of the cells emitting 10-fold less counts/s than D283luc, animals that displayed a large primary parenchymal tumor, indicative of a failed lateral ventricle injection, were excluded from the final survival comparison.

Immunohistochemistry was performed on the brains and spinal cords of MV-treated animals to definitively demonstrate MV dissemination and infection of D425luc tumor cells located throughout the CSF. Positive MV infection of medulloblastoma cells was located in the ventricles (Fig. 5A and B), posterior fossa (Fig. 5C and D), and the spinal cord (Fig. 5E and F), demonstrating MV infection of tumor cells distant from the site of inoculation. MV infection is associated with syncytia that were immunoreactive. The majority of the virus is located in the cytoplasm of infected cells. Untreated animals showed no immunoreactivity for MV (Fig. 5G–L) and negative controls performed by omitting the primary antibody revealed no staining (data not shown). Similar results were observed in D283luc MV-treated xenografts (data not shown). Subsequent staining demonstrated that the syncytia immunoreactive for MV in both the brain and the spinal cord also stained positive for cleaved caspase-3, a marker for apoptosis (Fig. 6A and B). Although there was a low level of apoptosis in the untreated samples (Fig. 6C and D), there was increased apoptosis in the MV-treated samples (Fig. 6A and B). Evaluation of the tumors from MV-infected and uninfected animals revealed a similar proliferation index, as assessed by Ki-67 staining (Fig. 6E–H). Review of MV-infected samples indicated that syncytia positive for MV and apoptosis immunoreactivity were negative for Ki-67 staining (Fig. E and F).

Discussion

Although advances in treatment modalities have increased the survival of children who receive a diagnosis of medulloblastoma, ~20% of these patients will present with disseminated disease and face a much worse prognosis. Because of the limitations and significant drawbacks associated with conventional therapy, alternative means for treating all variants of medulloblastoma are sorely needed. The decision to investigate the use of a modified Edmonston strain measles virus (MV-Edm) to treat disseminated medulloblastomas was motivated by several key observations. First, the oncolytic activity of the MV-Edm has already been demonstrated across multiple tumor types, where it has displayed remarkable specificity for targeting and destroying transformed cells, leaving the normal surrounding tissue intact.[19,22–24] Second, the general safety of the Edmonston vaccine strain has been thoroughly vetted over several decades of clinical use, having been safely administered to >1 billion recipients worldwide. Although a routine vaccination is certainly far removed from using a virus to treat a brain tumor, it should be noted that extensive studies with the latter

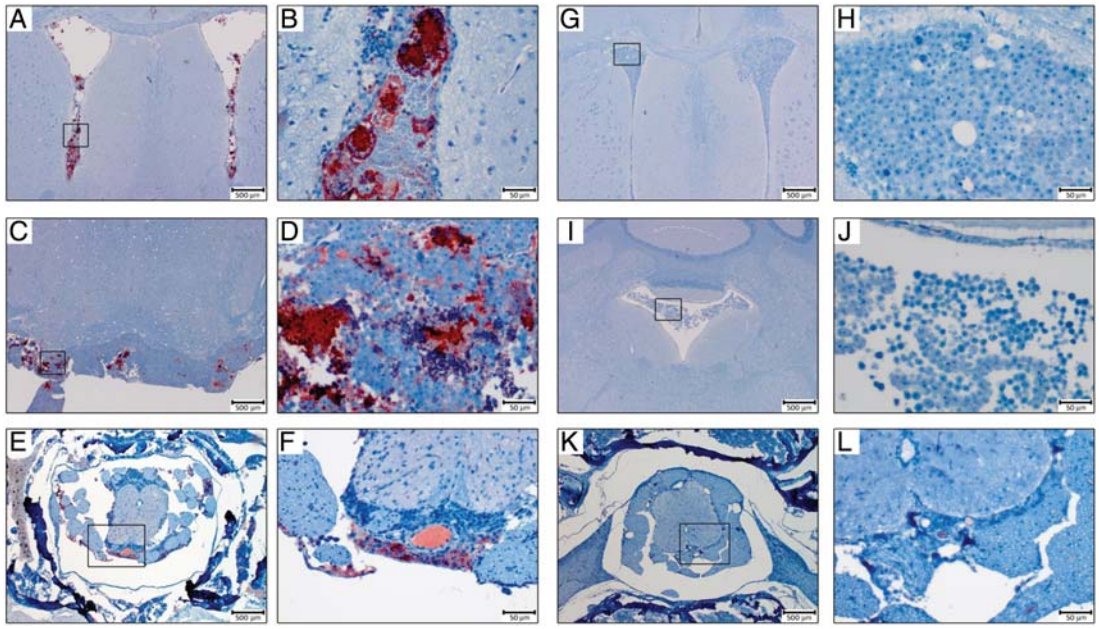

Fig. 5. Immunohistochemical measles virus (MV) detection. Paraffin-embedded tissue sections derived from D425luc xenografts were stained with a rabbit polyclonal MV nucleoprotein antibody. Nucleoprotein immunoreactivity was detected in the cytoplasm of individual cells and multi-nucleated syncytia. Positive MV infection of medulloblastoma cells was located in the ventricles (A and B), posterior fossa (C and D), and spinal cord (E and F) of MV-treated animals, but was not detected in untreated control animals (G–L).

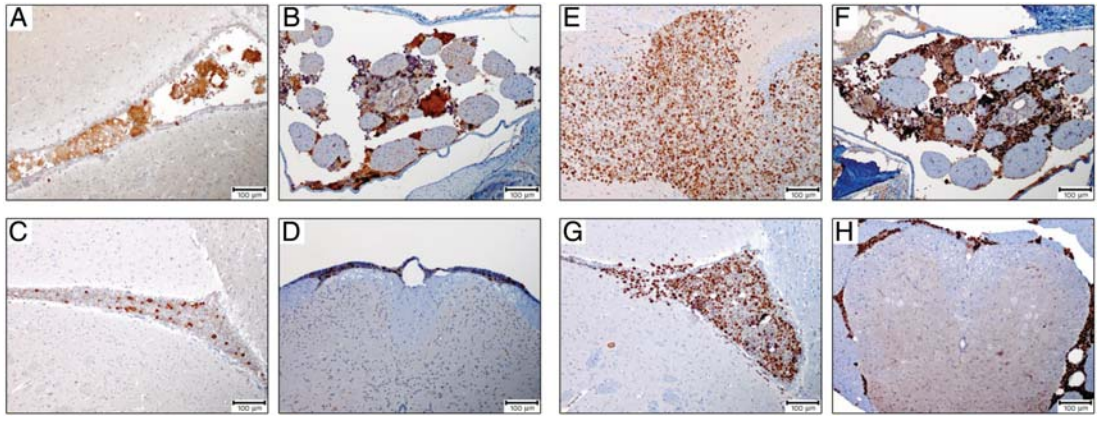

Fig. 6. Immunohistochemical apoptosis and cell proliferation staining. Paraffin-embedded tissue sections derived from D425luc xenografts were stained with either a rabbit polyclonal cleaved caspase-3 antibody, to detect apoptosis or a rabbit polyclonal Ki-67 to detect cell proliferation. Syncytia in both the brain and spinal cord stained positive for cleaved caspase-3 (A and B). While there was a low level of apoptosis in the untreated samples (C and D), there was increased apoptosis in the MV-treated samples (A and B). Tumors from MV-infected and non-infected animals revealed a similar proliferation index (E–H). Review of MV-infected samples indicated that syncytia positive for MV and apoptosis staining were negative for Ki-67 staining (E and F).

route of administration have already been conducted in nonhuman primates. In the early 1970s, Albrecht et al. found no clinical signs of encephalitis in rhesus monkeys following intracerebral injection with low-passage Edmonston strain virus.[25] In addition, no histological evidence of active measles infection, such as intranuclear inclusions or syncytia, could be found in any of the animals. Similarly, injection of Edmonston strain virus into the thalamus or CSF via cisternal injection of grivet monkeys or cynomologuous monkeys had no clinical toxicity.[26] Lastly, prior to initiating clinical trials for patients with glioblastoma multiforme, measles neurotoxicty studies were performed in previously immunized rhesus macaques.[27] Similar to previous safety studies, there was no evidence of toxicity in the animals, thereby demonstrating the safety of measles virus therapy. We recently reported on the efficacy of MV therapy in increasing the survival of mouse xenografts of human medulloblastoma.[17] In that study, we were able to show that MV was effective in treating

localized tumors in the caudate putamen. Animals treated with recombinant MV showed drastic reductions in tumor size, compared with animals that had received a UV-inactivated form of the virus and, consequently, increased overall survival. In addition, we demonstrated that bioluminescent imaging was a very effective and accurate method to evaluate tumor response to MV therapy. Although MV efficacy was performed on medulloblastoma cell lines, immunohistochemical evaluation of fresh, primary medulloblastoma resection specimens demonstrated that they express CD46, thus indicating that MV virotherapy may be useful clinically.[17]

To determine whether MV treatment efficacy would extrapolate to disseminated disease, we developed a mouse model that recapitulated the dissemination pattern of human medulloblastoma and allowed us to use intravital biolumniscent imaging to monitor tumor response to treatment. In this study, we demonstrated that implantation of human medulloblastoma cells directly into the CSF via the lateral ventricle generated bioluminescent signals in the head and spine of animals (Fig. 1). Subsequent histopathological evaluation revealed tumor deposits in the intraventricular space, intracranial subarachnoid space, and spinal subarachnoid space (Fig. 2), thus confirming our bioluminescent images.

Although we were able to accurately determine dissemination (Fig. 1) and follow tumor response to MV treatment (Fig. 2) using bioluminescent imaging, comparison of D283luc and D425luc cells reveal some of the limitations associated with intravital imaging. There is a lower limit of sensitivity. In vitro analysis and in vivo imaging revealed that D283luc cells emit 10-fold more photons/s. This was clearly demonstrated by the average spinal cord signal intensities initially observed in D283luc and D425luc xenografts (1.47×10^4 and 1.47×10^3 photons/s/cm^2/sr, respectively) and the time required past tumor implantation to observe a signal in the spinal cords. Attempts are currently being made to construct a D425luc cell line that emits increased photons/second/cell.

We were able to show that MV, when administered either 3 or 14 days following D283luc tumor implantation, significantly enhanced survival of animals with disseminated medulloblastoma (Fig. 4A and B). We were also able to demonstrate a significant increase in survival of animals implanted with D425luc, when MV treatment was initiated 3 days following tumor implantation but not when treatment was initiated 14 days following tumor implantation (Fig. 4C). Pathological comparison of tumor burden at 14 days and 3 days revealed increased tumor burden in the ventricles and concomitant enhanced dilation of the ventricles, including the fourth ventricle. The presence of hydrocephalus suggests that the tumor was impeding the flow of CSF from the ventricle to the subarachnoid space, therefore diminishing the access of MV to disseminated tumor sites. Our findings from initiating treatment 3 days following tumor implantation and 14 days following tumor implantation indicate that there may be a window for optimal MV treatment efficacy. Although we believe that tumor burden, especially in the ventricles, affected efficacy in our animal models, we do not believe this will be an issue when treating children. Although children with medulloblastoma often present with hydrocephalus, this is almost always caused by the tumor in the fourth ventricle, which is removed surgically prior to the institution of therapy.

Equally as important as the increase in animal survival using MV was the detection of MV infection at multiple tumor deposits throughout the subarachnoid space, including the spinal cord (Fig. 5). As expected, multi-nucleated giant cell syncytia were seen in the treated tumors, which were positive for MV when examined immunohistochemically. Further investigation determined that the syncytia associated with MV infection stained positive for cleaved caspase-3, a marker of apoptosis (Fig. 6A and B). The formation of syncytia and subsequent apoptosis has been well documented for MV.[24,28] In addition, both MV-treated and untreated animals displayed similar cell proliferation profiles as determined by Ki-67 staining (Fig. 6E–H). Evidence of MV infection confirmed our interpretation of the bioluminescent imaging data, which showed a decrease in signal intensity in MV-treated animals. As bioluminescent signal intensity was used as a surrogate marker of tumor burden, immunohistochemistry strongly suggests that MV is responsible for the decrease in tumor burden. The ability to use the CSF to deliver therapeutic MV to disseminated disease and to demonstrate infection at these distant sites is critical to treating mice and, ultimately, children presenting with disseminated disease.

Although other studies have been successful at generating disseminated disease in mouse models of medulloblastoma, either by metastasis from a primary tumor[15,16] or by direct injection into the subarachnoid space,[14] they required histological examination to determine whether they were successful at generating dissemination. The model that we present here has the advantage of using bioluminescent medulloblastoma cells, whose location and growth can be serially monitored without the need to sacrifice the animal. Moreover, this ensures consistency by eliminating from the study any animals that do not demonstrate dissemination prior to treatment. An additional advantage to this model is the ability to follow our treatment response. We are able to follow tumor growth, regression, and even dissemination from the brain to the spinal cord, allowing us to evaluate our MV efficacy in more detail and to know exactly when an animal is tumor free. As such, our model allows for more dynamic treatment regimens to be implemented. Animals can conceivably be treated as needed, receiving as little or as much MV as necessitated, depending on how they respond to treatment.

There are clinical challenges associated with MV therapy. The majority of patients eligible for MV therapy will have preexisting antiviral antibodies because of prior immunization or natural infection. However, there are methods available that circumvent or modulate the immune response against MV.

In studies investigating the therapeutic potential of herpesvirus and reovirus, the addition of the immunosuppressive agent cyclophosphamide prolonged viral gene expression and enhanced the oncolytic viral effect.[29–32] Another mechanism currently being developed to circumvent antimeasles immunity is cell-based carriers, such as mesenchymal stem cells.[33] This mechanism would allow delivery of MV to the tumor while evading the immune system.

In summary, we demonstrated that inoculation of MV directly into the CSF via the lateral ventricle significantly increased the survival of animals presenting with disseminated medulloblastoma. Intravital bioluminescent imaging provided a means by which disseminated medulloblastoma could be evaluated and a method to monitor tumor response to MV therapy. Evidence of MV infection at tumor deposits distant from the site of MV inoculation, concomitant with an increase in animal survival, demonstrated that modified MV has therapeutic potential for disseminated medulloblastoma. Additional studies, including evaluating the toxicity of MV injection directly into the CSF of previously immunized, immunocompetent, nonhuman primates will need to be completed prior to using the virus in a clinical trial for the treatment of disseminated medulloblastoma. Furthermore, the broad tropism toward varying malignancies, as evidenced by the ongoing clinical trials,[34–36] suggest that MV may be a viable therapeutic strategy toward other pediatric tumors (i.e., ependymomas and diffuse intrinsic potine gliomas). Studies are currently being performed to evaluate this treatment approach.

Acknowledgments

We thank the Core Morphology Laboratory and the Small Animal Imaging Facility of The Research Institute at Nationwide Children's Hospital for technical support.

Conflict of interest statement. None declared.

Funding

This work was supported by Nationwide Children's Hospital (start-up to C.R.).

References

1. Humphreys R. Posterior cranial fossa brain tumors in children. In: Youmans, J., ed. Neurological Surgery. Philadelphia: WB Saunders, 1982:2733–2752.
2. Bleyer WA. The impact of childhood cancer on the United States and the world. *CA Cancer J Clin*. 1990;40:355–367.
3. Allen JC, Bloom J, Ertel I, et al. Brain tumors in children: current cooperative and institutional chemotherapy trials in newly diagnosed and recurrent disease. *Semin Oncol*. 1986;13:110–122.
4. Hughes EN, Shillito J, Sallan SE, et al. Medulloblastoma at the joint center for radiation therapy between 1968 and 1984. The influence of radiation dose on the patterns of failure and survival. *Cancer*. 1988;61:1992–1998.
5. Palmer SL, Goloubeva O, Reddick WE, et al. Patterns of intellectual development among survivors of pediatric medulloblastoma: a longitudinal analysis. *J Clin Oncol*. 2001;19:2302–2308.
6. Freeman CR, Taylor RE, Kortmann RD, et al. Radiotherapy for medulloblastoma in children: a perspective on current international clinical research efforts. *Med Pediatr Oncol*. 2002;39:99–108.
7. Gurney JG, Kadan-Lottick NS, Packer RJ, et al. Endocrine and cardiovascular late effects among adult survivors of childhood brain tumors: Childhood Cancer Survivor Study. *Cancer*. 2003;97:663–673.
8. Ris MD, Packer R, Goldwein J, et al. Intellectual outcome after reduced-dose radiation therapy plus adjuvant chemotherapy for medulloblastoma: a Children's Cancer Group study. *J Clin Oncol*. 2001;19:3470–3476.
9. Inakoshi H, Kayamori R, Tsuchida E, et al. Multivariate analysis of dissemination relapse of medulloblastoma and estimation of its time parameter for craniospinal irradiation. *Radiat Med*. 2003;21:37–45.
10. Packer RJ. Childhood medulloblastoma: progress and future challenges. *Brain Dev*. 1999;21:75–81.
11. Zeltzer PM, Boyett JM, Finlay JL, et al. Metastasis stage, adjuvant treatment, and residual tumor are prognostic factors for medulloblastoma in children: conclusions from the Children's Cancer Group 921 randomized phase III study. *J Clin Oncol*. 1999;17:832–845.
12. Ellison DW, Clifford SC, Gajjar A, et al. What's new in neuro-oncology? Recent advances in medulloblastoma. *Eur J Paediatr Neurol*. 2003;7:53–66.
13. Packer RJ. Brain tumors in children. *Arch Neurol*. 1999;56:421–425.
14. Shimato S, Natsume A, Takeuchi H, et al. Human neural stem cells target and deliver therapeutic gene to experimental leptomeningeal medulloblastoma. *Gene Ther*. 2007;14:1132–1142.
15. Lun XQ, Zhou H, Alain T, et al. Targeting human medulloblastoma: oncolytic virotherapy with myxoma virus is enhanced by rapamycin. *Cancer Res*. 2007;67:8818–8827.
16. Yang WQ, Senger D, Muzik H, et al. Reovirus prolongs survival and reduces the frequency of spinal and leptomeningeal metastases from medulloblastoma. *Cancer Res*. 2003;63:3162–3172.
17. Studebaker AW, Kreofsky CR, Pierson CR, et al. Treatment of medulloblastoma with a modified measles virus. *Neuro Oncol*. 2010;12:1034–1042.
18. Duprex WP, McQuaid S, Hangartner L, et al. Observation of measles virus cell-to-cell spread in astrocytoma cells by using a green fluorescent protein-expressing recombinant virus. *J Virol*. 1999;73:9568–9575.
19. Phuong LK, Allen C, Peng KW, et al. Use of a vaccine strain of measles virus genetically engineered to produce carcinoembryonic antigen as a novel therapeutic agent against glioblastoma multiforme. *Cancer Res*. 2003;63:2462–2469.
20. Troy T, Jekic-McMullen D, Sambucetti L, et al. Quantitative comparison of the sensitivity of detection of fluorescent and bioluminescent reporters in animal models. *Mol Imaging*. 2004;3:9–23.
21. Northcott PA, Korshunov A, Witt H, et al. Medulloblastoma Comprises Four Distinct Molecular Variants. *J Clin Oncol*. 2010;29:1408–1414.

22. Grote D, Russell SJ, Cornu TI, et al. Live attenuated measles virus induces regression of human lymphoma xenografts in immunodeficient mice. *Blood*. 2001;97:3746–3754.
23. Peng KW, Ahmann GJ, Pham L, et al. Systemic therapy of myeloma xenografts by an attenuated measles virus. *Blood*. 2001;98:2002–2007.
24. Peng KW, TenEyck CJ, Galanis E, et al. Intraperitoneal therapy of ovarian cancer using an engineered measles virus. *Cancer Res*. 2002;62:4656–4662.
25. Albrecht P, Shabo AL, Burns GR, et al. Experimental measles encephalitis in normal and cyclophosphamide-treated rhesus monkeys. *J Infect Dis*. 1972;126:154–161.
26. Buynak EB, Peck HM, Creamer AA, Goldner H, Hilleman MR. Differentiation of virulent from avirulent measles strains. *American Journal of Diseases of Children*. 1962;103:460–473.
27. Myers R, Harvey M, Kaufmann TJ, et al. Toxicology study of repeat intracerebral administration of a measles virus derivative producing carcinoembryonic antigen in rhesus macaques in support of a phase I/II clinical trial for patients with recurrent gliomas. *Hum Gene Ther*. 2008;19:690–698.
28. Esolen LM, Park SW, Hardwick JM, et al. Apoptosis as a cause of death in measles virus-infected cells. *J Virol*. 1995;69:3955–3958.
29. Fulci G, Breymann L, Gianni D, et al. Cyclophosphamide enhances glioma virotherapy by inhibiting innate immune responses. *Proc Natl Acad Sci USA*. 2006;103:12873–12878.
30. Fulci G, Dmitrieva N, Gianni D, et al. Depletion of peripheral macrophages and brain microglia increases brain tumor titers of oncolytic viruses. *Cancer Res*. 2007;67:9398–9406.
31. Ikeda K, Ichikawa T, Wakimoto H, et al. Oncolytic virus therapy of multiple tumors in the brain requires suppression of innate and elicited antiviral responses. *Nat Med*. 1999;5:881–887.
32. Tyminski E, Leroy S, Terada K, et al. Brain tumor oncolysis with replication-conditional herpes simplex virus type 1 expressing the prodrug-activating genes, CYP2B1 and secreted human intestinal carboxylesterase, in combination with cyclophosphamide and irinotecan. *Cancer Res*. 2005;65:6850–6857.
33. Mader EK, Maeyama Y, Lin Y, et al. Mesenchymal stem cell carriers protect oncolytic measles viruses from antibody neutralization in an orthotopic ovarian cancer therapy model. *Clin Cancer Res*. 2009;15:7246–7255.
34. Galanis E, Hartmann LC, Cliby WA, et al. Phase I trial of intraperitoneal administration of an oncolytic measles virus strain engineered to express carcinoembryonic antigen for recurrent ovarian cancer. *Cancer Res*. 2010;70:875–882.
35. NCT00390299. Viral Therapy in Treating Patients with Recurrent Glioblastoma. 2008 [cited; Available from: http://www.clinicaltrials.gov/ct2/show/NCT00390299.
36. NCT00450814. Vaccine Therapy with or without Cyclophosphamide in Treating Patients with Recurrent or Refractory Multiple Myeloma. 2008 [cited; Available from: http://www.clinicaltrials.gov.ct2/show/NCT00450814.